Prepublished copy

Nature Environment & Pollution Technology

This is a peer-reviewed prepublished version of the paper to be published in Vol. 25, No. 1, March 2026 issue

Original Research

Assessing Water Quality through Remote Sensing: A Regression-Based Approach with Sentinel-2 Data

Mridul S. Seth[1]†, Mrugen B. Dholakia[1], Sanjay D. Dhiman[2], Umesh. K. Khare[3] , Jignesh A. Amin[4], Pranavkumar Bhangaonkar[5] and Dipika Shah[6]

[1]Gujarat Technological University, Ahmedabad-382424, Gujarat, India

[2]Birla Vishvakarma Mahavidyalaya, Vallabh Vidyanagar, Anand-388120, Gujarat, India

[3]Government Engineering College, Shamlaji Road, Aravali District, Modasa-383315, Gujarat, India

[4]GTU-School of Engineering and Technology, Ahmedabad-382424, Gujarat, India

[5]Neotech Faculty of Diploma Engineering, Vadodara-384435, Gujarat, India

[6]Shree Swaminarayan Institute of Technology, Gandhinagar-382428, Gujarat, India

†Corresponding author: Mridul S. Seth; wowsethg@gmail.com

ORCID IDs of Authors

Mridul S Seth: https://orcid.org/0000-0003-4662-6175

Dr. Sanjay D Dhiman: https://orcid.org/0000-0002-4392-6503

Dr. Jignesh A Amin: https://orcid.org/0000-0002-9374-6092

Dr. Pranavkumar Bhangaonkar: https://orcid.org/0000-0001-6925-8796

Key Words	Remote sensing, Google earth engine, Regression modeling, GIS, Water quality monitoring
DOI	https://doi.org/10.46488/NEPT.2026.v25i01.B4340 (DOI will be active only after the final publication of the paper)
Citation for the Paper	Seth, M.S., Dholakia, M.B., Dhiman, S., Khare, U.K., Amin, J., Bhangaonkar, P. and Shah, D., 2026. Assessing water quality through remote sensing: A regression-based approach with Sentinel-2 data. *Nature Environment and Pollution Technology*, 25(1), p. B4340. https://doi.org/10.46488/NEPT.2026.v25i01.B4340

ABSTRACT

Monitoring water quality is essential for human health and environmental sustainability. Traditional methods relying on laboratory analysis and point-based sampling often lack sufficient spatial and temporal coverage. This study assessed water quality along the Sabarmati Riverfront in Ahmedabad, India, using Google Earth Engine (GEE) and Sentinel-2 satellite imagery. Key parameters such as pH, turbidity (Tur), Electrical Conductivity (EC), Total Suspended Solids (TSS), Total Solids (TS), Dissolved Oxygen (DO), Biochemical Oxygen Demand (BOD), Total

Phosphorus (TP), Fecal Coliform (FC), and Ammonia (NH_3) were estimated through remote sensing. An empirical regression model was developed to relate in-situ data to satellite-derived spectral indices. The results revealed significant seasonal and spatial variations, with some areas displaying favorable levels of TSS, BOD, and FC. The model exhibited strong predictive accuracy for pH, TSS, and TP (R^2 = 0.80, R^2 = 0.76, R^2 = 0.75 respectively), and moderate performance for turbidity (R^2 = 0.62). The integration of remote sensing and GIS enables scalable, cost-effective, real-time water quality monitoring, offering critical insights for pollution control and water resource management. Future research should explore hyperspectral imaging and machine learning to enhance predictive accuracy and broaden the applicability of satellite-based monitoring models.

INTRODUCTION

1.1 Background information

Water is a vital resource for sustaining life on Earth and significantly contributes to the economic and social development of nations (Ingrao *et al.* 2023). It plays a central role across various sectors, including industrial and domestic infrastructure, agriculture, recreation, navigation, and water storage systems (Bănăduc et al. 2022). Ensuring water quality through regular and continuous monitoring is essential for informed and timely decision-making in water resource management (Kapalanga *et al.* 2021). However, water quality can vary substantially across geographical regions, necessitating the consideration of both its quantity and quality in strategic planning processes (Kumar *et al.* 2024). Accurate and real-time data accessibility is therefore crucial for the effective distribution and planning of water resources at regional scales (Imiya et al. 2023).

The integration of cloud computing platforms with advanced predictive models has demonstrated the potential to enhance decision-making efficiency in water management systems (Sherjah *et al.* 2023). Traditional water quality monitoring approaches, which rely heavily on point-based sampling and laboratory analyses, are limited by their spatial and temporal coverage. These methods are not only time-intensive and costly but also inadequate for capturing the dynamic behaviour of water bodies, particularly in remote or large-scale areas (Adjovu *et al.* 2023; Essamlali *et al.* 2024). Consequently, there is a growing need for more comprehensive, real-time monitoring systems capable of supporting effective environmental governance.

Water quality is typically determined by a range of chemical, physical, and biological parameters (Misman *et al.* 2023). Among these, certain physical and chemical attributes such

as chlorophyll-a, turbidity, and coloured dissolved organic matter (CDOM) are classified as optically active parameters (Fu *et al.* 2022), while others—including dissolved oxygen (DO), total nitrogen (TN), and total phosphorus (TP)—are considered non-optical parameters (Gao *et al.* 2024). Remote sensing (RS) platforms equipped with optical and thermal sensors—mounted on boats, aircraft, or satellites—offer both spatial and temporal data for environmental monitoring (Kanjir *et al.* 2018). These technologies have increasingly been applied to monitor variations in water quality and to support the development of improved water management strategies (Adjovu *et al.* 2023).

Recent studies have advanced the development of algorithms aimed at estimating optically active water quality parameters using RS data (Yang *et al.* 2022). For example, (Maciel *et al.* 2023) compared regional retrieval algorithms with established models, evaluating the efficacy of Sentinel-2 MultiSpectral Instrument (MSI) indices in extracting chlorophyll-a concentrations in optically complex aquatic environments. Similarly, (Bonansea *et al.* 2019) demonstrated that satellite-derived spectral indices exhibit strong correlations within situ measurements of optically active water quality parameters. These findings underscore the potential of satellite data for operational water quality assessment, particularly when coupled with machine learning techniques (Najafzadeh et al. 2023).

The continuous evolution of cloud computing, machine learning, and big data analytics has marked a transformative shift in environmental monitoring practices (Chi et al. 2016; Di et al. 2023). Authors (Chen *et al.* 2022) have provided a comprehensive evaluation of remote sensing big data frameworks and techniques, focusing on water extraction and quantitative water quality estimation. These advances enable the characterization of multispectral signals, which reflect the hydrological, biological, and chemical attributes of water bodies as well as the physical properties of the surrounding environment. Spectral data in the 0.36 µm to 2.36 µm range, particularly within the visible and near-infrared bands (0.4–0.9 µm), have shown promising capabilities for detecting water contaminants via their spectral signatures (Seyhan et al. 1986). Further exploration of machine learning applications for estimating non-optically active parameters is discussed in the subsequent literature review section.

Unlike previous studies that focused on regional or global models, this study uniquely integrates Google Earth Engine (GEE) with regression analysis to estimate water quality parameters for the Sabarmati River, enabling scalable and efficient monitoring in a data-limited context.

1.2 Literature Review

Effective monitoring of inland water quality is essential for managing eutrophication, pollution, and ecological degradation, especially in areas experiencing intensified anthropogenic activity and climate variability. In recent years, remote sensing (RS) has emerged as a valuable tool for observing water quality parameters (WQPs) over broad spatial and temporal scales, complementing or even replacing traditional in-situ methods in certain contexts. The integration of RS with field measurements has proven effective in capturing spatially distributed information on key indicators such as Total Suspended Solids (TSS), Total Nitrogen (TN), Total Phosphorus (TP), Chemical Oxygen Demand (COD), and chlorophyll-a. For example, (Muhoyi *et al.* 2022) demonstrated the use of Sentinel-2 imagery in conjunction with in-situ sampling to map eutrophication-related contaminants in Zimbabwe's Lower Manyame Sub-catchment (LMS), identifying upstream sources of pollution and highlighting nutrient-driven degradation. Similar approaches have been applied in Egypt's Timsah Lake (Seleem *et al.* 2022) and India's Renuka Lake (Jally *et al.* 2024), revealing long-term eutrophic conditions exacerbated by anthropogenic pressures.

Despite these advances, satellite-based monitoring of inland water systems faces technical limitations, such as low signal-to-noise ratios, atmospheric interference, and coarse resolution in narrow or heterogeneous water bodies. To mitigate these issues, researchers have incorporated proximal remote sensing techniques. For instance, (Sun *et al.* 2022) developed empirical algorithms based on spectral reflectance and in-situ concentrations of COD, TN, and TP from multiple sites in China, achieving model accuracies exceeding 80–90%. These hybrid techniques improve precision while retaining broader observational advantages. Parallel to sensor improvements, the adoption of statistical and machine learning methods has enhanced retrieval accuracy and interpretability of WQPs. Studies employing multivariate analyses, such as principal component analysis (PCA) and varimax rotation, have been instrumental in identifying dominant pollution factors, including industrial discharge and ion exchange dynamics, as seen in the Daman Ganga River (Seth *et al.* 2025) and groundwater systems in Patna (Zafar *et al.* 2024). Moreover, artificial intelligence models, including recurrent neural networks (RNNs) and ARIMA forecasting methods, have been proposed to dynamically predict coastal water quality using RS data (Bodapati 2023).

Comprehensive reviews as presented in Table 1 further illustrate the expanding role of RS in water quality monitoring. These studies categorize RS methods into empirical, semi-empirical, analytical, and machine learning-based approaches and emphasize the use of both optical and microwave sensors for retrieving parameters such as colored dissolved organic matter (CDOM), turbidity, TSM, and chlorophyll-a (Yang *et al.* 2022; Adjovu *et al.* 2023). The

increased availability of hyperspectral sensors and unmanned aerial vehicles (UAVs) has further enhanced spatial and spectral resolution, enabling near-real-time assessments.

However, standardization challenges remain. Variability in Water Quality Index (WQI) computation methods—such as those applied in the Aksu and Kali rivers (Şener et al. 2017; Said et al. 2021) — limits cross-regional comparisons and the operational use of RS data in policymaking. Addressing these inconsistencies requires improved model calibration, regional adaptation of algorithms, and harmonized data reporting frameworks. Recent assessments (e.g., (Tsitsi et al. 2024)) advocate for deeper integration of RS with ground observations, enhanced sensor calibration, and algorithm optimization. These steps are crucial to overcome current limitations and realize the full potential of RS for continuous, accurate, and scalable water quality monitoring in support of environmental sustainability.

Table 1: Represents the comparative literature review

Source	Approach	WQ Parameters	Accuracy Assessment	Method
(Muhoyi *et al.* 2022)	RS: Sentinel-2	TSS, TP, TN, COD	R^2 Range: 0.63 – 0.78	Empirical Models
(Sun *et al.* 2022)	Proximal Remote Sensing	TN, TP, COD	R^2 Range: 0.84–0.93	Empirical & Machine Learning Models
(Seleem *et al.* 2022)	RS: Sentinel-2 and Landsat-8	Total Suspended Matter, Chlorophyll-a	Ground truth data was not available	Empirical and Semi-Analytical Models
(Maciel *et al.* 2023)	RS: Sentinel 2	Chlorophyll-a	R^2 Range: 0.77 – 0.98	Empirical Models
(Zhang *et al.* 2021)	RS: Sentinel 2 and Sentinel 3	Water Quality Index	R^2 Range: 0.69 - 0.81	Machine Learning Models
(Jally *et al.* 2024)	RS: Landsat 8 & LISS III	Secchi Disk Transparency & Trophic State Index	$R^2 = 0.94$	Regression Models
(Zafar *et al.* 2024)	GIS with Conventional Approach	11 WQ Parameters	Poor WQI	PCA, HCA and Interpolation Technique
(Seth *et al.* 2025)	Conventional Approach	17 WQ Parameters	Poor WQI	PCA followed by Factor Analysis

RS: Remote Sensing

1.3 Contextualizing the objectives

The main objective of this work is to present a methodology that requires remote sensing for the evaluation of the variation in water characteristic as pH, Electrical Conductivity (EC), Turbidity (Tur), Total Suspended Solids (TSS), Total Solids (TS), Biochemical Oxygen Demand (BOD), Dissolved Oxygen (DO), Total Phosphorus (TP), Fecal Coliform (FC), and Ammonia (NH_3) via a regression model and the GEE platform. With that purpose, the intention was as follows:

- To use different indices and band ratios for water quality determination via Sentinel–2 satellite images,
- The Google Earth Engine (GEE) platform is used to obtain satellite images and their processing is used to evaluate the water characteristics,
- Analysis of inland water body located in the Sabarmati Riverfront, Ahmedabad, Gujarat, India,
- Regression model is used to determine the relationships among field data and remote sensing data.

2. MATERIALS AND DATA

2.1 Study Area

The Sabarmati Riverfront is located at the coordinates of Latitude: 23.0341367°N and Longitude:72.5723255°E. The Sabarmati Riverfront is a waterfront developed along the banks of the Sabarmati River in Ahmedabad, India as shown in Figure 1. Since 2012 the waterfront has been gradually opened to public as facilities are constructed. The riverbed land is reclaimed on both the east and west banks to construct an around 11.25 kilometer long riverfront. The project aims to provide Ahmedabad with a meaningful waterfront environment along the banks of the Sabarmati River and to redefine the identity of Ahmedabad around the river. The average annual rainfall in Ahmedabad city is approximately 782 mm.

2.2 Field Data

Field data were collected from 5 sites along the Sabarmati Riverfront as shown in Figure 2 at a depth of 1 m from the water surface. The samples were collected by keeping the standards to follow from collection to transportation to storage until the experiment was conducted. The physical and chemical characteristics of water, such as pH, Electrical Conductivity (EC), Turbidity (Tur), Total Suspended Solids (TSS), Total Solids (TS), Biochemical Oxygen Demand (BOD), Dissolved Oxygen (DO), Total Phosphorus (TP), Fecal Coliform (FC), and Ammonia (NH_3) were determined in the NABL Accredited laboratory at Ahmedabad, India. The samples were collected on three dates of the months February-March-April 2024 as represented in Table 2.

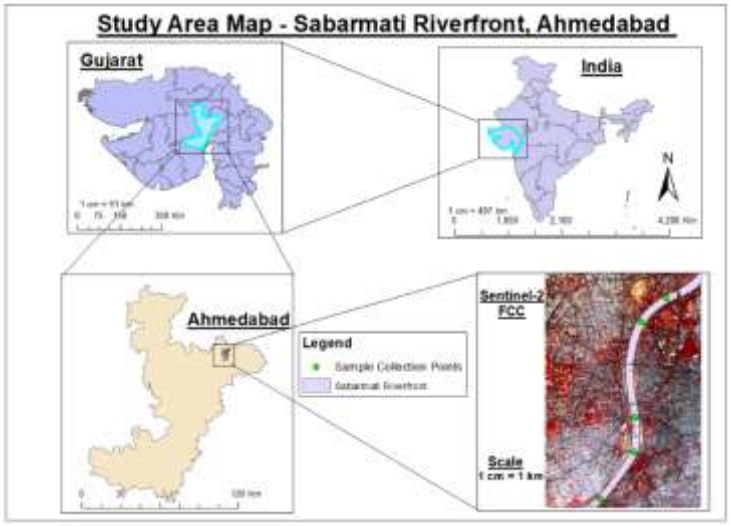

Figure 1: Study Area Map of Sabarmati Riverfront showing with Sentinel – 2 FCC satellite image of Sabarmati Riverfront.

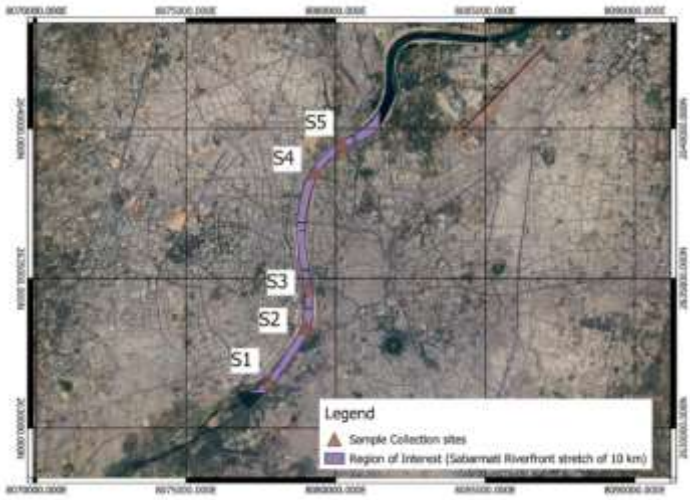

Figure 2: Representing the sample collection sites over approximately 10 km Sabarmati Riverfront, Ahmedabad as a region of interest.

2.3 Satellite Data (Google Earth Engine)

Google Earth Engine (GEE) is used by various researchers and integrates real-world applications and visualizations of geospatial datasets through the application of algorithms to map, identify and measure variations on Earth's surface, for real world applications (Haifa *et al.* 2020; Pham-Duc *et al.* 2023; Velastegui-Montoya *et al.* 2023). In a study conducted by the (Pérez-Cutillas *et al.* 2023), the most prevalent methodological uses of GEE (22%) were for the evaluation and prediction of water resources. The imagery data collected from the Sentinel-2 satellite with spatial resolution of 10m for B2 (Band 2 with Blue Color bandwidth) , B3 (Band 3 with Green Color bandwidth), B4 (Band 4 with Red Color bandwidth) and B8 (Band 8 with

Near Infrared bandwidth) were used, to evaluate the water characteristics in line with the field collection data sample dates, as shown in Table 3.

Table 2: Represents the sample collected for the water quality parameters

S. No.	Abbreviation	Parameters	Unit
1	pH	pH	pH Units
2	Tur	Turbidity	mg/L
3	EC	Electrical Conductivity	µmho/cm
4	TSS	Total Suspended Solids	mg/L
5	TS	Total Solids	mg/L
6	BOD_5	Biochemical Oxygen Demand of 5 days	mg/L
7	DO	Dissolved Oxygen	mg/L
8	TP	Total Phosphorous	mg/L
9	FC	Fecal Coliform	mg/L
10	NH_3	Ammonia	mg/L

Table 3: Representing the dates of sample collection through Field and Satellite

Field Sample Collection Date	08th Feb 2024	09th March 2024	10th April 2024
Satellite Image Collection Date	06th Feb 2024	07th March 2024	06th April 2024

3. METHODOLOGY

3.1 Approach (Relationships between remote-sensing and field-based water quality parameters)

Many studies have been conducted with combinations of various bands either individually or as ratios of the entire visible wavelength region to monitor the variation in the spectral response (Doxaran *et al.* 2005; Vakili and Jamil 2020). The present study was performed with the band range from Blue to NIR to monitor the variation in the spectral response due to a change in the various water parameters.

The methodology can be categorized into three major stages as represented in Table 4 and Figure 3. This study illustrated a decision-making system for water quality monitoring with Sentinel-2 satellite images using Google Earth Engine (GEE) platform, with a particular emphasis on temporal and spatial fluctuations along Ahmedabad's Sabarmati Riverfront. The Sentinel-2 data were obtained in February, March, and April of 2024, ensuring that the dates of the imagery corresponded with the dates of the collection of water samples. This made it possible to precisely record seasonal fluctuations in the quality of the water. Five different

locations along the Sabarmati Riverfront were used for the study to capture the spatial heterogeneity in the river's water properties as shown in Figure -2.

Table 4: Represents the main stages for the determination of Water Quality Parameter.

Stage	Description
1	Use the GEE platform to filter images from Sentinel 2 collections of February 2024, March 2024 and April 2024 sync with the in-situ sample collection dates.
2	Applying water index NDWI to automatically identify the water surface that qualifies for processing using the GEE platform.
3	Evaluate the water quality parameters value for each valid image by applying the developed correlation expression using pixel values of various bands and their combination with field measured data through regression model.

The primary phase of the procedure is to access and pre-process Sentinel-2 imagery for the chosen months of 2024 via the Google Earth Engine (GEE) platform. With its 13 spectral bands, Sentinel-2's Multispectral Instrument (MSI) is especially well-suited for tracking important water quality metrics, with this study focusing on 10 water quality parameters as shown in Table 2.

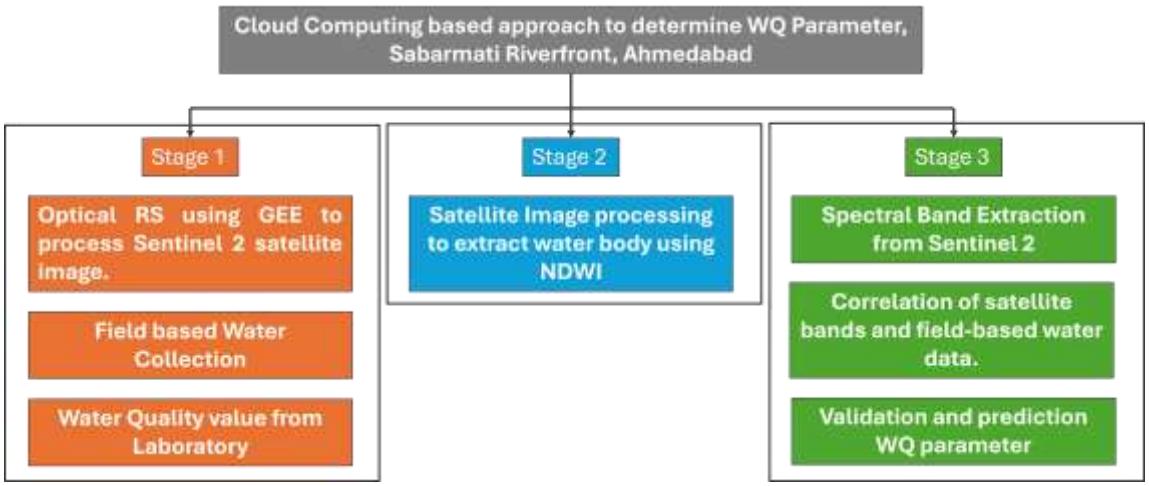

Figure 3: A broad framework of methodology

3.2 Regression model using spectral properties

By examining the spectral reflectance characteristics of satellite images, remote sensing technology offers an effective way to estimate water quality indicators. Sentinel-2 provides useful information for developing correlations between spectral indices and indicators of water quality because of its multispectral bands. The spectral properties of the water body are extracted and analyzed using zonal statistics, which compute the statistical values as the mean, median, standard deviation, variance, minimum and maximum of the reflectance values for the various bands as B2, B3, B4, and B8 bands along with the combination of bands such as B2/B3,

Normalized Differential Water Index (NDWI) & Normalized Differential Turbidity Index (NDTI) spectral band at all 5 stations. The zonal statistics were extracted based on the considered region near each station of sample collection as shown in Table 5.

$$NDWI = (B3 - B8) / (B3 + B8) \quad \ldots(i)$$

$$NDTI = (B4 - B3) / (B4 + B3) \quad \ldots(ii)$$

Table 5: Representing the area of polygon plotted to extract zonal statistics at various stations

Polygon Station	S1	S2	S3	S4	S5
Area (m^2)	41063.853	40519.885	28578.369	50656.604	46731.693

These mean values of reflectance were used as data inputs to create empirical models. Furthermore, a correlation study was performed to determine the relationship between the spectral data obtained from the satellite and the 10 water characteristics measured in the laboratory. Field samples were taken at each of the five locations along the Sabarmati Riverfront throughout the designated months to obtain ground truth data for water characteristics.

The linear regression model can be created via the Data Analysis tool in Microsoft Excel after the data has been organized, with each parameter being modeled separately. The output consists of an R^2 value that indicates the goodness of fit of the model and regression coefficients that show how each spectral band contributes to the prediction of the water quality metrics. Higher R^2 values indicate a more robust correlation between the reflectance data and the parameter being modeled for water quality as shown in Table 6. Empirical models based on this association are then used to forecast water characteristic concentrations throughout the study area by applying them to spectral data. The created expressions are utilized to estimate water characteristic concentrations within the GEE, and the results are mapped and displayed to produce spatially explicit water quality information.

By comparing the estimates obtained from satellite data with independent ground truth data of water characteristics, the precision of these predictions is validated. The models' performance is evaluated by computing the statistical metric R^2. Modifications are applied as needed to improve the models' prediction power. Using Sentinel-2 imagery through the Google Earth Engine, this system captures both spatial fluctuations along Ahmedabad's Sabarmati Riverfront and temporal fluctuations over the designated months, demonstrating the effective and scalable application of these tools for water quality monitoring. This approach offers insightful information for regional environmental management and decision-making.

Table 6: Representing the correlation expression developed using measured ground truth data and mean spectral reflectance values

S. No.	**Parameters**	**Expressions**

1.	pH	$31.46 - 0.0296 \times B2 + 0.0584 \times B3 - 0.0226 \times B4 - 0.0088 \times B8 - 22.446 \times \left(\frac{B3}{B2}\right) - 16.97 \times NDWI + 52.249 \times NDTI$
2.	Turbidity	$-2311.71 + 2.0317 \times B2 - 2.284 \times B3 + 0.60877 \times B4 - 0.0448 \times B8 + 1968.82 \times \left(\frac{B3}{B2}\right) - 441.042 \times NDWI - 2052.5 \times NDTI$
3.	Electrical Conductivity	$9007.85 - 7.87 \times B2 + 10.2 \times B3 - 3.86 \times B4 + 0.529 \times B8 - 7764.93 \times \left(\frac{B3}{B2}\right) + 1207.43 \times NDWI + 9502.98 \times NDTI$
4.	Total Suspended Solids	$-536.082 + 0.68294 \times B2 - 1.45326 \times B3 + 3.21347 \times B4 - 2.2606 \times B8 - 5338.93 \times NDWI - 7511.93 \times NDWI - 7511.8 \times NDTI + 392.034 \times (\frac{B3}{B2})$
5.	Total Solids	$-791.931 - 45318.7 \times NDTI - 15.8 \times B8 - 40432 \times NDWI + 16.65 \times B4$
6.	BOD_5	$159.613 - 0.2488 \times B2 - 0.52 \times B3 + 1.577 \times B4 - 0.802 \times B8 - 177.88 \times \left(\frac{B3}{B2}\right) - 2053.87 \times NDWI - 4061.06 \times NDTI$
7.	DO	$-2681.63 + 2.33 \times B2 - 3.524 \times B3 + 1.879 \times B4 - 0.3 \times B8 + 2249.49 \times B3/B2 - 945.11 \times NDWI - 4727.05 \times NDTI$
8.	Total Phosphorous	$419.5 - 0.372 \times B2 + 0.624 \times B3 + 0.0057 \times B4 - 0.31 \times B8 - 358.8 \times B3/B2 - 760.23 \times NDWI - 71.325 \times NDTI$
9.	Fecal Coliform	$1090.826 - 1.14 \times B2 + 1.414 \times B3 + 1.56 \times B4 - 1.97 \times B8 - 944.97 \times \frac{B3}{B2} - 4997.83 \times NDWI - 4323.97 \times NDTI$
10.	Ammonia (NH_3)	$628.69 - 0.577 \times B2 + 0.655 \times B3 - 0.036 \times B4 - 0.114 \times B8 - 547.31 \times B3/B2 - 303.51 \times NDWI + 36.87 \times NDTI$

4. RESULTS AND DISCUSSION

4.1 Relationships between remote-sensing data and field-based water quality parameters

The geospatial images of the Sentinel-2 satellite data are utilized to depict the geographical distributions of the water quality metrics in three separate months (2024): February, March, and April. A crucial resource for evaluating the temporal and geographical changes in the river's water quality along the Sabarmati Riverfront is provided in this section. Figure 4 for Optically Active Water Characteristics & Figure 5 for Non-Optically Active Water Characteristics, depict the distributions of these images, which show important patterns associated with both natural and human-caused processes, as well as fluctuations in each water characteristic. A deeper and thorough examination of each figure is given in Table 7 for Optically Active Water Characteristics and in Table 8 for the Non-Optically Active Water Characteristics, with particular attention given to the trends in spatial distribution and any possible ramifications for the management of water resources.

Table 7: Represents the comparative analysis of Optically Active Water Characterstics.			
Parameter	**Months**	**Observations**	**Key Insights**
EC	February	Increased EC readings in several river segments, point to the possible presence of dissolved salts.	• Salinity and pollution from dissolved ions are well-indicated by EC. • Management methods should concentrate on reducing salt levels, particularly during peak runoff times, as reflected by the seasonal changes in EC.
	March	The conductivity somewhat decreased, presumably because of early rainfall dilution, although there are still some isolated hotspots.	
	April	Increased EC readings in several river segments, point to the possible presence of dissolved salts.	
Turbidity	February	Significant increases in suspended particle matter.	• Excessive turbidity frequently signals problems with water quality, including decreased light penetration, which endangers aquatic life. • Decreasing level indicating that some sedimentation had taken place.
	March	The turbidity level has somewhat decreased, indicating that some sedimentation has taken place.	
	April	The turbidity values are relatively modest, suggesting cleaner water	
TSS	February	TSS levels exhibit a decreasing trend from February to April, peaking in certain zones, especially in February.	•Decrease in TSS have the potential to less severely harm aquatic ecosystems by suffocating habitats, increasing photosynthesis, and causing nutrient overload (Bilotta and Brazier 2008).
	March		
	April		
TS	February	The high TS levels are indicative of runoff and pollution sources' suspended particulates as well as their dissolved salts	•TS distribution also exhibits a pattern similar to that of the TSS •High TS can deteriorate the quality of water for ecological and drinking reasons (Saalidong *et al.* 2022).
	March	The chart for March shows some respite in the dissolved loads.	
	April	Hotspot zones, especially in April, might be related to runoff or human activity upstream of the riverfront.	

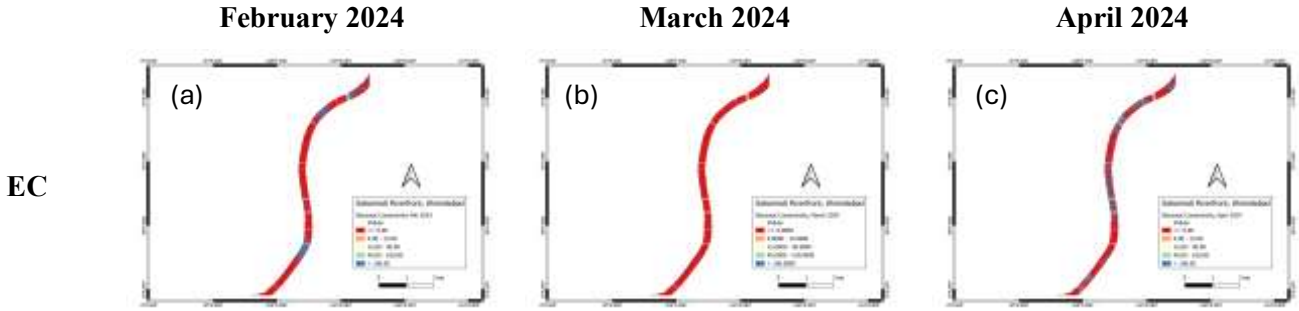

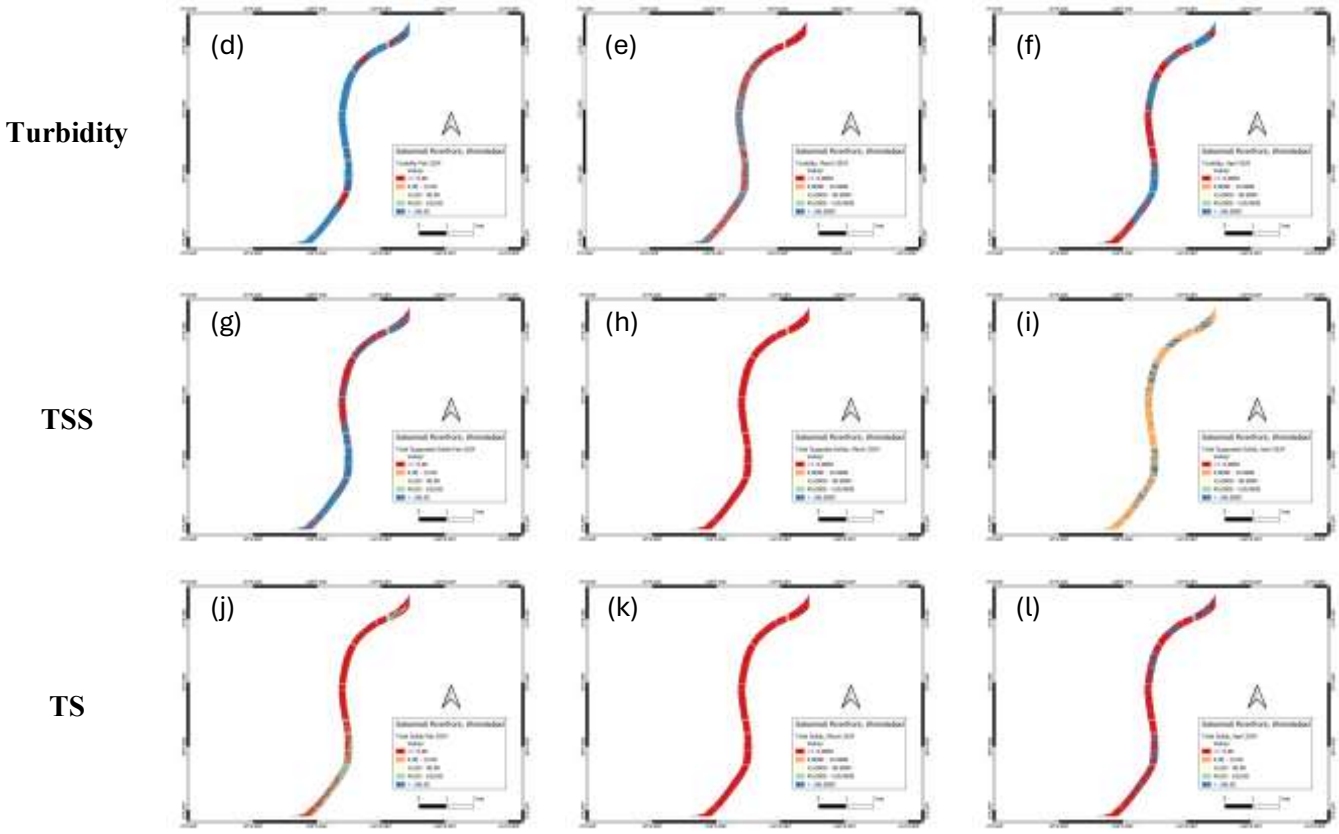

Figure 4: Represents the spatial distribution of Optically Active Water Characterstics

Table 8: Represents the comparative analysis of Non-Optically Active Water Characterstics.

Parameter	Months	Observations	Key Insights
pH	February	The pH distribution seems very regular in February, indicating a steady chemical composition on the other side of the river.	•pH levels fluctuate, ranging from almost neutral to slightly alkaline. •Small pH variations indicate chemical contamination or increased runoff in the early stages, thus places exhibiting these changes should be regularly watched to prevent additional damage.
	March	Shows some geographical variation, especially in places where urban runoff could affect the quality of the water	
	April	Slight alkalinity increases in temperature as April approaches may be a sign of increased biological activity	
BOD	February	Rising BOD levels point to organic material entering the river	• The observed BOD levels are low, and, in few cases, they are below the detection level according to the data collected from the field. • Aquatic lives are not endangered by decreased BOD levels because they maintain the amount of oxygen in the water (Chapra *et al.* 2021).
	March	In summer time organic pollution is suggested by the low March and April readings.	
	April		

DO	February	A lower BOD level can correlate with higher DO levels as lower organic matter breaks down and less oxygen is consumed, resulting in the spatially defined oxygen zones observed in these months.	• Across the three months, higher DO levels correlated with lower BOD levels. • (Nugraha *et al.* 2020). suggests lower organic input treatments are necessary, particularly in warmer months when oxygen depletion might be more severe
	March		
	April		
TP	February	Comparatively more levels of TP dispersion are observed in February.	• Elevated total phosphorus levels are a major cause of algal blooms, which can severely deteriorate the quality of water (Li *et al.* 2022).
	March		
	April		
FC	February	A considerable increase in fecal coliform levels was observed, especially in upstream areas, which suggests that rainwater runoff or raw sewage are the main possible causes	•These results highlight how crucial it is to enhance water treatment strategies and management, where intake structures are planned to be placed to avoid overloading pollution. •Seasonal increases in FC point to possible threats to human health, particularly in locations where the river is used for leisure (Guangzhi *et al.* 2022).
	March	March's comparatively low FC readings indicate that contamination may have been lower during the month's dry spell.	
	April	A considerable increase in fecal coliform levels was observed.	
NH_3	February	The elevated levels in February might indicate increasing nutrient contamination.	•Aquatic life may be poisoned by high ammonia levels (Edwards *et al.* 2024).
	March	Low spatial distribution of ammonia in the March & April month.	
	April		

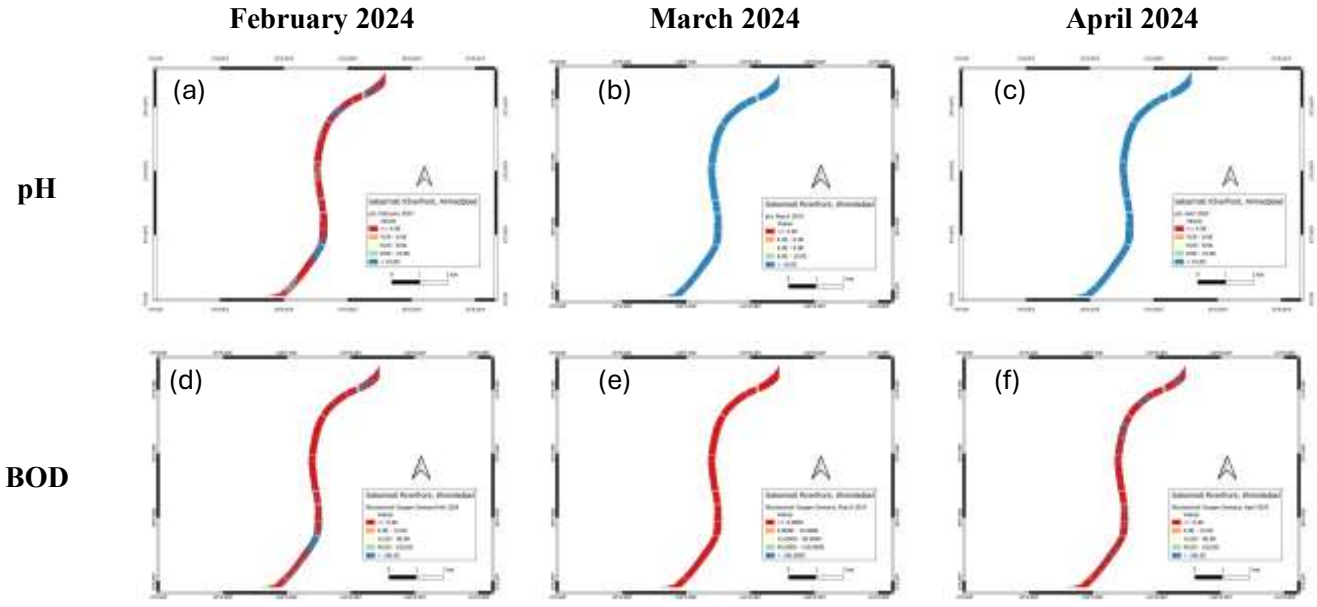

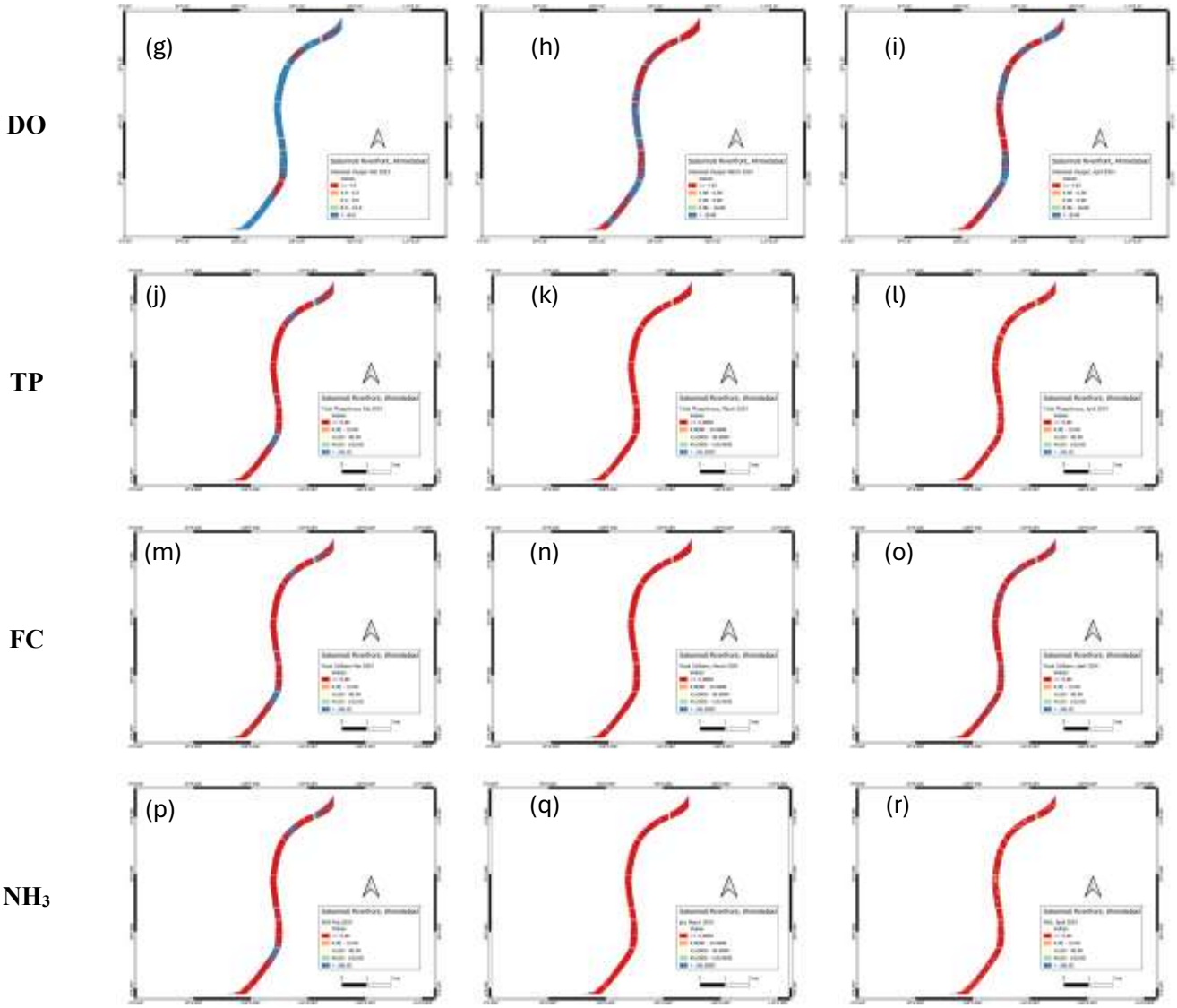

Figure 5: Represents the spatial distribution of Non-Optically Active Water Characterstics.

4.2 OVERALL ANALYSIS

The spatial representations highlight the distribution of important water quality indicators, such as pH, turbidity, EC, Total Suspended Solids (TSS), Total Solids (TS), Total Phosphorous (TP), Fecal Coliform (FC), Biochemical Oxygen Demand (BOD), Dissolved Oxygen (DO), and Ammonia (NH3). For tracking changes over time, each satellite image is shown for a particular date of every three months. Effective management of water resources and identification of pollution sources is made possible by this temporal analysis, which provides thorough knowledge of how water quality metrics change over the course of many seasons.

- The satellite imagery of February 2024 shows that certain metrics, such as pH and EC, have rather uniform distributions, but other parameters, including TSS and turbidity,

show more localized variability. The maps show places that need more research as possible hotspots for pollution where specific characteristics differ from typical values.

- There appears to be a shift in the distribution of water quality in the images from March 2024, which might be attributed to fluctuations in seasonal patterns, human activities, or rainfall. The influence of runoff and biomass, for example, appears to be reflected in the fluctuations in turbidity and TSS concentrations, particularly in populated areas along the riverside.
- The geographical patterns of water quality metrics continue to evolve by April. Desirable levels of BOD, FC, and NH_3 in particular regions might indicate stable or lower pollution levels. On the other hand, certain regions have relatively high DO levels, suggesting the potential for effective interventions or natural healing processes.

An extensive dataset for comprehending the spatial and temporal variations in the water quality of the Sabarmati Riverfront is created on the basis of geospatial images of its characteristics. Anthropogenic activities including biomass, and urban runoff are the main causes of the notable seasonal fluctuations that are observed across numerous parameters, notably between the months of February, March, and April. These deep insights identify regions that need targeted management measures and highlight key times when water quality is most in danger. The status of the river system can be considered healthy and may be maintained by water resource management by addressing the causes of pollution and putting targeted measures into place in the future.

4.3 ACCURACY ASSESSMENT

It is crucial to test the model's performance with a fresh dataset after it has been calibrated. As a result, the model revealed positive forecast parameters related to water quality in various scenarios such as pH with $R^2 = 0.8$; TP with $R^2 = 0.75$; and TSS with $R^2 = 0.76$. The model offers an economical and effective way to continuously monitor water quality by applying it to Sentinel-2 images taken at different times after it has been validated.

The estimations of various parameters produced from satellite data are compared with experimentally observed values to validate the water quality prediction model. Graphics are used as shown in Figure 6, to visualize the comparison and offer insights into the model's performance across various parameters, including pH, Turbidity, Electrical Conductivity (EC), Total Suspended Solids (TSS), Total Solids (TS), Dissolved Oxygen (DO), Biochemical Oxygen Demand (BOD), Total Phosphorus (TP), Fecal Coliform (FC), and Ammonia (NH_3). When assessing the degree to which the model's predictions and the actual measurements agree, the R^2 values are essential. The general connection between the expected and actual values is

shown by the trend line in each graph, which provides information about the linearity and dependability of the model.

A strong match is shown by the R^2 value of 0.802, which shows that the model explains 80.2% of the variation in pH. Past studies have shown a positive relationship and high accuracy in evaluating the Remote Sensing based derived pH (Pereira *et al.* 2020; Jiang *et al.* 2022). With an R^2 of 0.38, the EC graph indicates that 38% of the variation in EC can be explained by the model, demonstrating a weak connection between the observed and predicted values. The turbidity graph, with R^2 of 0.58, indicates a moderate correlation between the observed and expected values. The model accounts for 58% of the turbidity variability, suggesting that it accurately describes the overall trend but has difficulty explaining very murky waters. The model accounts for 76.5% of the variability in the TSS, according to the TSS validation graph, which has a strong R^2 of 0.765. The Total Solids (TS) graph's R^2 value is 0.621. Although the trend line is almost straight, it exhibits a slightly underestimated at higher TS levels, much like the TSS. The model's inability to fully capture the extent of organic pollution is indicated by the BOD graph, which has R^2 of 0.362 and indicates lower predictive accuracy. The trend line in the validation graph for DO underestimates the concentration of Dissolved Oxygen in low-oxygen areas but fits rather well at higher oxygen levels, with a modest R^2 value of 0.614. R^2 of 0.747 indicates a strong association in the TP validation graph. The model accounts for 45.1% of the variability in FC levels, according to the Fecal Coliform graph, which has an R^2 of 0.451. The validation graph for Ammonia (NH_3) has a R^2 value of 0.31, again suggesting a lower level of model performance.

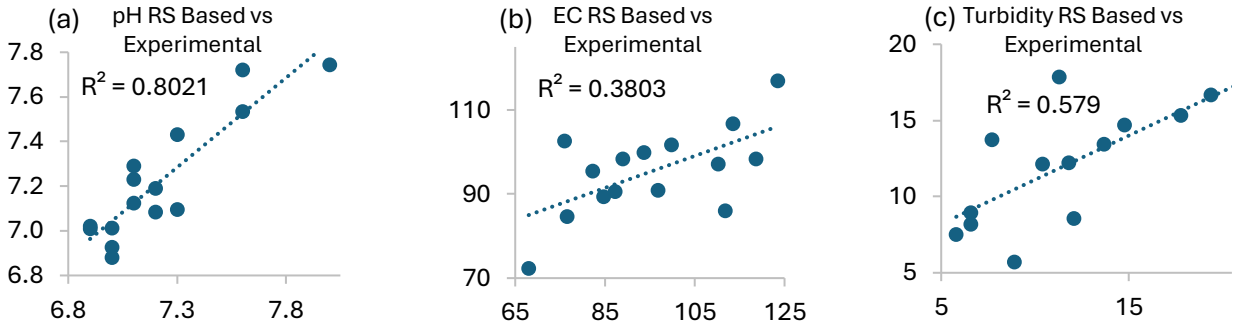

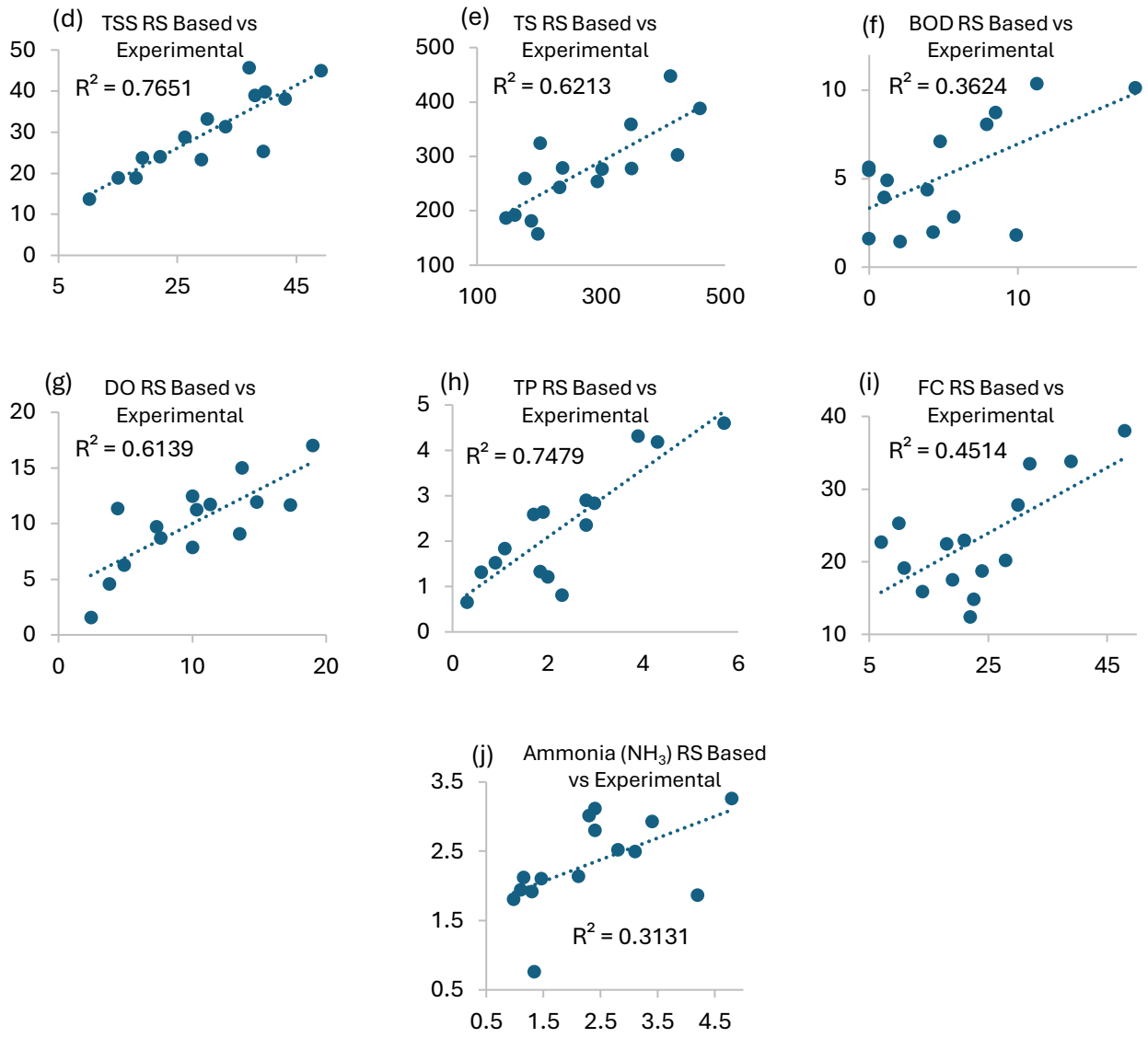

Figure 6: R^2 values for accuracy assessment of Remote-Sensing derived V/s Experimental water quality concentrations.

Table 9: Summarizing R^2 for all parameters

S. R. No.	Parameters	R^2 Range	Classification
1.	pH, TSS, TP,	>0.7	Good
2.	Turbidity, TS, DO,	0.5 – 0.7	Moderate
3.	EC, BOD, FC, NH_3	<0.5	Weak

The validation findings demonstrate as in Table 9, that the model performs well for a variety of parameters, including pH, TSS, and TP, with R^2 values often over 0.7, suggesting a robust match. Nevertheless, the model displays more notable departures from the trend line for parameters such as NH_3, BOD, FC, and DO, with R^2 values ranging from 0.31 to 0.62, indicating the need for greater refinement. The trend line study shows that although the model performs well in most situations when there is a high concentration of physical contaminants,

it finds it difficult to represent linear connections in other instances. As a result, even if the model works well for assessing water quality generally, further calibration or the use of nonlinear modeling approaches would be required to enhance forecasts in regions with more severe environmental circumstances. The model's prediction accuracy over a wider variety of scenarios might be greatly improved by including more advanced regression techniques or machine learning algorithms.

5. CONCLUSIONS

This study validated the efficacy of an integrated strategy to assess water quality at Ahmedabad's Sabarmati Riverfront, utilizing both in situ measurements and remote sensing derived data. By using multitemporal, remote sensing data, natural resource managers can benefit from the integrated approach, which is an affordable technology that has been demonstrated to be a valuable source of data for defining the water quality status of Ahmedabad's Sabarmati Riverfront. Additionally, changes in water quality can be analyzed through cloud-based accessibility of the data, that can quickly aid in the assessment of environmental issues and possible health hazards. Municipal authorities may face challenges in selecting locations to develop water intake structures that supply water to treatment plants. The chosen location should ideally be on a river stretch with lower levels of pollution. Through this approach using GIS visualizations, authorities can identify spatial water quality indicators and select sites with the lowest pollution levels, ensuring a more effective and safer water supply.

The following future scope can be considered as the possibility, to develop a time series of monitoring water quality parameter data integrated with precipitation data and change detection in land-use-land-cover patterns for better decision making regarding the variation in water characteristics. Also, to enhance prediction accuracy, future studies can integrate machine learning algorithms such as Random Forest (RF) and Support Vector Regression (SVR) for handling high-dimensional spectral data with nonlinear relationships modeling between spectral indices and water quality parameters. Using remote sensing techniques, sediment transport and erosion patterns can also be studied to understand their effects on turbidity and total suspended solids. On the other hand, the limitations faced during the study are that the measured spectral reflectance data should be obtained after thorough spectroscopic experimental comparisons. However, the spectral range was considered to be multispectral Sentinel-2, whereas the correlation can be developed via hyperspectral remote sensing images. Real-time monitoring and analysis of water quality can help prevent pollution, safeguard ecosystems, and protect public health by enabling early detection of issues. This approach not

only aids in water quality assessment but also supports decision-making related to site suitability, offering a valuable tool for regional planning and management.

ACKNOWLEDGEMENT

The authors acknowledge the assistance provided by Gujarat Technological University through its Seed Money Scheme to successfully execute the funded research project.

DATA AVAILABILITY STATEMENT

The data that support the findings of this study are available upon reasonable request.

DECLARATION OF CONFLICTING INTERESTS

On behalf of all the authors, the corresponding author states that there are no conflicts of interest.

REFERENCES

Adjovu, G.E., Stephen, H., James, D., and Ahmad, S. (2023) 'Overview of the Application of Remote Sensing in Effective Monitoring of Water Quality Parameters', *Remote Sensing*, 15(7), available: https://doi.org/10.3390/rs15071938.

Bănăduc D, Simić V, Cianfaglione K, Barinova S, Afanasyev S, Öktener A, McCall G, Simić S, C.-B.A. (2022) 'Freshwater as a Sustainable Resource and Generator of Secondary Resources in the 21st Century: Stressors, Threats, Risks, Management and Protection Strategies, and Conservation Approaches', available: https://doi.org/10.3390/ijerph192416570.

Bilotta, G. and Brazier, R. (2008) 'Understanding the Influence of Suspended Solids on Water Quality and Aquatic Biota', *Water research*, 42, 2849–2861, available: https://doi.org/10.1016/j.watres.2008.03.018.

Bodapati, G.J.L.S.S.B. and T.S.P. V. (2023) 'Water Quality Monitoring Using Remote-Sensing', available: https://doi.org/10.1109/CISES58720.2023.10183395.

Bonansea, M., Ledesma, M., Rodriguez, C., and Pinotti, L. (2019) 'Using new remote sensing satellites for assessing water quality in a reservoir', *Hydrological Sciences Journal*, 64(1), 34–44, available: https://doi.org/10.1080/02626667.2018.1552001.

Chapra, S.C., Camacho, L.A., and McBride, G.B. (2021) 'Impact of global warming on dissolved oxygen and bod assimilative capacity of the world's rivers: Modeling analysis', *Water (Switzerland)*, 13(17), available: https://doi.org/10.3390/w13172408.

Chen, J., Chen, S., Fu, R., Li, D., Jiang, H., Wang, C., Peng, Y., Jia, K., and Hicks, B.J. (2022) 'Remote Sensing Big Data for Water Environment Monitoring: Current Status, Challenges, and Future Prospects', *Earth's Future*, 10(2), 1–33, available: https://doi.org/10.1029/2021EF002289.

Chi, M., Plaza, A., Benediktsson, J.A., Sun, Z., Shen, J., and Zhu, Y. (2016) 'Big Data for Remote Sensing: Challenges and Opportunities', *Proceedings of the IEEE*, 104(11), 2207–2219, available: https://doi.org/10.1109/JPROC.2016.2598228.

Di, L. and Yu, E. (2023) 'Big Data Analytics for Remote Sensing: Concepts and Standards BT - Remote Sensing Big Data', in Di, L. and Yu, E., eds., Cham: Springer International Publishing, 155–170, available: https://doi.org/10.1007/978-3-031-33932-5_9.

Doxaran, D., Cherukuru, R.C.N., and Lavender, S.J. (2005) 'Use of reflectance band ratios to estimate suspended and dissolved matter concentrations in estuarine waters', *International Journal of Remote Sensing*, 26(8), 1763–1769, available: https://doi.org/10.1080/01431160512331314092.

Edwards, T.M., Puglis, H.J., Kent, D.B., Durán, J.L., Bradshaw, L.M., and Farag, A.M. (2024) 'Ammonia and aquatic ecosystems – A review of global sources, biogeochemical cycling, and effects on fish', *Science of the Total Environment*, 907(October 2023), available: https://doi.org/10.1016/j.scitotenv.2023.167911.

Essamlali, I., Nhaila, H., and El Khaili, M. (2024) 'Advances in machine learning and IoT for water quality monitoring: A comprehensive review', *Heliyon*, 10(6), e27920, available: https://doi.org/10.1016/j.heliyon.2024.e27920.

Fu, B., Lao, Z., Liang, Y., Sun, J., He, X., Deng, T., He, W., Fan, D., Gao, E., and Hou, Q. (2022) 'Evaluating optically and non-optically active water quality and its response relationship to hydro-meteorology using multi-source data in Poyang Lake, China', *Ecological Indicators*, 145(November), available: https://doi.org/10.1016/j.ecolind.2022.109675.

Gao, L., Shangguan, Y., Sun, Z., Shen, Q., and Shi, Z. (2024) 'Estimation of Non-Optically Active Water Quality Parameters in Zhejiang Province Based on Machine Learning', *Remote Sensing*, 16(3), 1–19, available: https://doi.org/10.3390/rs16030514.

Guangzhi, X., Tao, W., Yao, W., Yunxia, Z., and Jialuo, C. (2022) 'Fecal coliform distribution and health risk assessment in surface water in an urban-intensive catchment', available: https://doi.org/10.1016/j.jhydrol.2021.127204.

Haifa, T., Bahram, S., Masoud, M., Lindi, Q., Sarina, A., and Brian, B. (2020) 'Google Earth Engine for geo-big data applications: A meta-analysis and systematic review', available: https://doi.org/https://doi.org/10.1016/j.isprsjprs.2020.04.001.

Imiya M. Chathuranika, Erandi Sachinthanie, Phub Zam, Miyuru B. Gunathilake, Denkar Denkar, Nitin Muttil, Amila Abeynayaka, Komali Kantamaneni, Upaka Rathnayake (2023) 'Assessing the water quality and status of water resources in urban and rural areas of Bhutan', available: https://doi.org/https://doi.org/10.1016/j.hazadv.2023.100377]/.

Ingrao, C., Strippoli, R., Lagioia, G., and Huisingh, D. (2023) 'Water scarcity in agriculture: An overview of causes, impacts and approaches for reducing the risks', *Heliyon*, 9(8), e18507, available: https://doi.org/10.1016/j.heliyon.2023.e18507.

Jally, S.K., Kumar, R., and Das, S. (2024) 'Integrating Satellite Data and In-situ Observations for Trophic State Assessment of Renuka Lake, Himachal Pradesh, India', *Nature Environment and Pollution Technology*, 23(4), 2025–2038, available: https://doi.org/10.46488/NEPT.2024.v23i04.010.

Jiang, Z., Song, Z., Bai, Y., He, X., Yu, S., Zhang, S., and Gong, F. (2022) 'Remote Sensing of Global Sea Surface pH Based on Massive Underway Data and Machine Learning', *Remote Sensing*, 14(10), 1–24, available: https://doi.org/10.3390/rs14102366.

Kanjir, U., Greidanus, H., and Oštir, K. (2018) 'Vessel detection and classification from spaceborne optical images: A literature survey', *Remote Sensing of Environment*, 207(December 2017), 1–26, available: https://doi.org/10.1016/j.rse.2017.12.033.

Kapalanga, T.S., Hoko, Z., Gumindoga, W., and Chikwiramakomo, L. (2021) 'Remote-sensing-based algorithms for water quality monitoring in olushandja dam, north-central namibia', *Water Supply*, 21(5), 1878–1894, available: https://doi.org/10.2166/ws.2020.290.

Kumar, D., Kumar, R., Sharma, M., Awasthi, A., and Kumar, M. (2024) 'Global water quality indices: Development, implications, and limitations', *Total Environment Advances*, 9(December 2023), 200095, available: https://doi.org/10.1016/j.teadva.2023.200095.

Li, M., Li, Y., Zhang, Y., Xu, Q., Iqbal, M.S., Xi, Y., and Xiang, X. (2022) 'The significance of phosphorus in algae growth and the subsequent ecological response of consumers', *Journal*

of Freshwater Ecology, 37(1), 57–69, available: https://doi.org/10.1080/02705060.2021.2014365.

Maciel, F.P., Haakonsson, S., Ponce de León, L., Bonilla, S., and Pedocchi, F. (2023) 'Challenges for chlorophyll-a remote sensing in a highly variable turbidity estuary, an implementation with sentinel-2', *Geocarto International*, 38(1), available: https://doi.org/10.1080/10106049.2022.2160017.

Misman, N.A., Sharif, M.F., Chowdhury, A.J.K., and Azizan, N.H. (2023) 'Water pollution and the assessment of water quality parameters: a review', *Desalination and Water Treatment*, 294, 79–88, available: https://doi.org/10.5004/dwt.2023.29433.

Muhoyi, H., Gumindoga, W., Mhizha, A., Misi, S.N., and Nondo, N. (2022) 'Water quality monitoring using remote sensing, Lower Manyame Sub-catchment, Zimbabwe', *Water Practice and Technology*, 17(6), 1347–1357, available: https://doi.org/10.2166/wpt.2022.061.

Najafzadeh, M. and Basirian, S. (2023) 'Evaluation of River Water Quality Index Using Remote Sensing and Artificial Intelligence Models', *Remote Sensing*, 15(9), available: https://doi.org/10.3390/rs15092359.

Nugraha, W.D., Sarminingsih, A., and Alfisya, B. (2020) 'The Study of Self Purification Capacity Based on Biological Oxygen Demand (BOD) and Dissolved Oxygen (DO) Parameters', *IOP Conference Series: Earth and Environmental Science*, 448(1), available: https://doi.org/10.1088/1755-1315/448/1/012105.

Pereira, O.J.R., Merino, E.R., Montes, C.R., Barbiero, L., Rezende-Filho, A.T., Lucas, Y., and Melfi, A.J. (2020) 'Estimating water pH using cloud-based landsat images for a new classification of the Nhecolândia Lakes (Brazilian Pantanal)', *Remote Sensing*, 12(7), available: https://doi.org/10.3390/rs12071090.

Pérez-Cutillas, P., Pérez-Navarro, A., Conesa-García, C., Zema, D.A., and Amado-Álvarez, J.P. (2023) 'What is going on within google earth engine? A systematic review and meta-analysis', *Remote Sensing Applications: Society and Environment*, 29(September 2022), 100907, available: https://doi.org/10.1016/j.rsase.2022.100907.

Pham-Duc, B., Nguyen, H., Phan, H., and Tran-Anh, Q. (2023) 'Trends and applications of google earth engine in remote sensing and earth science research: a bibliometric analysis using scopus database', *Earth Science Informatics*, 16(3), 2355–2371, available: https://doi.org/10.1007/s12145-023-01035-2.

Saalidong, B.M., Aram, S.A., Otu, S., and Lartey, P.O. (2022) 'Examining the dynamics of the relationship between water pH and other water quality parameters in ground and surface water systems', *PLoS ONE*, 17(1 1), 1–17, available: https://doi.org/10.1371/journal.pone.0262117.

Said, S. and Khan, S.A. (2021) 'Remote sensing-based water quality index estimation using data-driven approaches: a case study of the Kali River in Uttar Pradesh, India', *Environment, Development and Sustainability*, 23(12), 18252–18277, available: https://doi.org/10.1007/s10668-021-01437-6.

Seleem, T., Bafi, D., Karantzia, M., and Parcharidis, I. (2022) 'Water Quality Monitoring Using Landsat 8 and Sentinel-2 Satellite Data (2014–2020) in Timsah Lake, Ismailia, Suez Canal Region (Egypt)', *Journal of the Indian Society of Remote Sensing*, 50(12), 2411–2428, available: https://doi.org/10.1007/s12524-022-01613-9.

Şener, Ş., Şener, E., and Davraz, A. (2017) 'Evaluation of water quality using water quality index (WQI) method and GIS in Aksu River (SW-Turkey)', *Science of the Total Environment*, 584–585, 131–144, available: https://doi.org/10.1016/j.scitotenv.2017.01.102.

Seth, M., Dholakia, M., Dhiman, S., Khare, U.K., Amin, J., and Bhangaonkar, P. (2025) 'Multivariate analysis of inland water quality index in parts of Vapi district, Gujarat, India', *Water Supply*, 25(2), 193–211, available: https://doi.org/10.2166/ws.2024.264.

Seyhan, E. and Dekker, A. (1986) 'APPLICATION OF REMOTE SENSING TECHNIQUES FOR WATER QUALITY MONITORING', *HYDROBIOLOGICAL BULLETIN*, 20(1/2), 83–94.

Sherjah, P.Y., Sajikumar, N., and Nowshaja, P.T. (2023) 'Quality monitoring of inland water bodies using Google Earth Engine', *Journal of Hydroinformatics*, 25(2), 432–450, available: https://doi.org/10.2166/hydro.2023.137.

Sun, X., Zhang, Y., Shi, K., Zhang, Y., Li, N., Wang, W., Huang, X., and Qin, B. (2022) 'Monitoring water quality using proximal remote sensing technology', *Science of the Total Environment*, 803, available: https://doi.org/10.1016/j.scitotenv.2021.149805.

Tsitsi Bangira, Trylee Nyasha Matongera, Tafadzwanashe Mabhaudhi, O.M. (2024) 'Remote sensing-based water quality monitoring in African reservoirs, potential and limitations of sensors and algorithms: A systematic review', available: https://doi.org/10.1016/j.pce.2023.103536.

Vakili, T. and Jamil, A. (2020) 'Determination of optically inactive water quality variables using Landsat 8 data: A case study in Geshlagh reservoir affected by agricultural land use', available: https://doi.org/doi.org/10.1016/j.jclepro.2019.119134.

Velastegui-Montoya, A., Montalván-Burbano, N., Carrión-Mero, P., Rivera-Torres, H., Sadeck, L., and Adami, M. (2023) 'Google Earth Engine: A Global Analysis and Future Trends', *Remote Sensing*, 15(14), available: https://doi.org/10.3390/rs15143675.

Yang, H., Kong, J., Hu, H., Du, Y., Gao, M., and Chen, F. (2022) 'A Review of Remote Sensing for Water Quality Retrieval: Progress and Challenges', *Remote Sensing*, 14(8), available: https://doi.org/10.3390/rs14081770.

Zafar, M.M., Sulaiman, M.A., and Kumari, A. (2024) 'GIS-Based Mapping of the Water Quality and Geochemical Assessment of the Ionic Behavior in the Groundwater Aquifers of Middle Ganga Basin, Patna, India', *Nature Environment and Pollution Technology*, 23(3), 1433–1447, available: https://doi.org/10.46488/nept.2024.v23i03.014.

Zhang, F., Chan, N.W., Liu, C., Wang, X., Shi, J., Kung, H. Te, Li, X., Guo, T., Wang, W., and Cao, N. (2021) 'Water quality index (Wqi) as a potential proxy for remote sensing evaluation of water quality in arid areas', *Water (Switzerland)*, 13(22), 1–17, available: https://doi.org/10.3390/w13223250.